

http://pubs.acs.org/journal/aesccq Article

# Efficient HO<sub>x</sub> Radical Production from Isoprene Nighttime Chemistry

Zeyi Moo, Peizhi Hao, Kate E. DeMarsh, and Xuan Zhang\*



Cite This: ACS Earth Space Chem. 2024, 8, 361–368



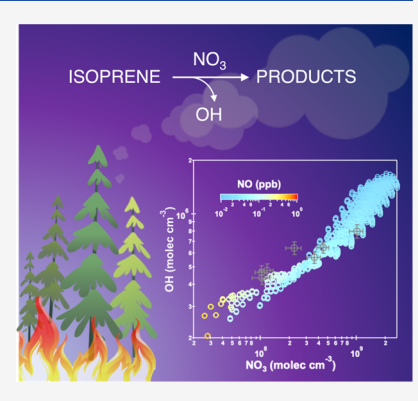
**ACCESS** I

Metrics & More

Article Recommendations

Supporting Information

ABSTRACT: The reactive chemistry of isoprene, the most emitted biogenic hydrocarbon worldwide, has a controlling influence on the composition and cleansing capacity of the atmosphere. Although isoprene emission by plant biosynthesis is negligible at night, heatstressed vegetation in close proximity to the fire front releases a substantial amount of isoprene, which subsequently reacts with  $NO_3$  radicals, the major oxidant in the dark. In this study, we performed chamber experiments to investigate the efficacy of  $HO_x$  recycling through the nighttime chemistry of isoprene. By operating the experiments at the continuous-flow steady-state mode, we created a chemical regime that features sub-ppbv levels of  $NO_3$  a regime that is highly relevant to the nighttime atmosphere disturbed by fire plumes but was rarely studied in previous chamber experiments. Using measurements of trace levels of cyclohexane at steady state, we derived the total OH radicals produced from isoprene +  $NO_3$  reactions in the range of  $(4.4-8.0) \times 10^5$  molecules cm<sup>-3</sup>, accounting for 9.9-17.7% of the total reacted isoprene mass. To explain this high level of observed OH, a



simplified mechanism that efficiently generates and converts  $HO_2$  to OH was proposed. By incorporating this mechanism into an observationally constrained box model, we predicted that the mixing ratio of OH radicals can exceed  $\sim 10^5$  molecules cm<sup>-3</sup> when isoprene and NO were present at parts per trillion by volume, a level frequently encountered in environments impacted by biomass burning emissions. Such an efficient production of OH radicals has an important impact on the oxidizing power of the nocturnal atmosphere in regions with intertwined biogenic and anthropogenic activities.

KEYWORDS: isoprene,  $NO_3$  oxidation, nighttime chemistry,  $HO_x$  generation, atmospheric oxidation capacity

# 1. INTRODUCTION

Oxidation of biogenic volatile organic compounds (BVOCs) by nitrate radicals (NO<sub>3</sub>) during nighttime represents one of the crucial interactions between biogenic emissions and anthropogenic pollution. NO<sub>3</sub> radical, a well-known nighttime tropospheric oxidant, is selectively reactive toward unsaturated hydrocarbons and serves as an important sink of BVOCs in the nocturnal atmosphere.<sup>2,3</sup> As the most abundant BVOC with global emissions of 440-660 Tg C yr<sup>-1,4</sup> the nighttime degradation of isoprene plays an important role in modulating the fate of reactive nitrogen within the continental boundary layer, initiating the recycling of hydrogen oxide radicals (HO<sub>x</sub>) at night, and perturbing the extent of photochemistry during the next day. Although isoprene emissions from plant biosynthesis at night are negligible, 6,7 heat-stressed vegetation in close proximity to the fire front releases a significant amount of isoprene, 8,9 which remains in the nighttime atmosphere at up to hundreds of ppt levels 10,11 and can be effectively removed by the reaction with NO3 radicals. 12,13 It has been estimated that 6-7% isoprene mass is oxidized in darkness globally, 14 consequently enhancing the secondary organic aerosols (SOA) production from isoprene by ~10%. 15

 $NO_3$ -initiated oxidation of isoprene proceeds predominantly by the  $NO_3$  addition to the carbon double bonds, with  $C_1$  addition favored over  $C_4$ . The lifetime of isoprene with respect to the reaction with  $NO_3$  is  $\sim 0.8$  h at typical ambient

 $NO_3$  mixing ratios of 5  $\times$  10<sup>8</sup> molecules cm<sup>-3</sup> at room temperature. Following the initial NO<sub>3</sub> attack, two separate pools of nitrooxy allylic radicals (1-ONO<sub>2</sub> and 4-ONO<sub>2</sub> adducts) are established, as displayed in Figure 1. Following collisional thermalization, nitrooxy allylic radicals add oxygen  $(O_2)$  at either  $\beta$  or  $\delta$  position to yield four distinct nitrooxy peroxy radicals ( $\beta$ -INOO and  $\delta$ -INOO), which further react with NO, NO<sub>3</sub>, HO<sub>2</sub>, and RO<sub>2</sub> radicals, producing an array of first-generation products that are primarily constituted by organic nitrates. <sup>18–20</sup> The oxidation of BVOCs by NO<sub>3</sub> has been recognized as an important source of nocturnal  $HO_x$  radicals. The role of  $NO_3$  as the  $HO_x$  radical propagator via the oxidation of isoprene has also been demonstrated by recent laboratory evidence. 20,24 In particular, a group of characteristic products generated from the OH-initiated oxidation of isoprene were observed in the isoprene + NO<sub>3</sub> reaction system. Mechanisms generating HO<sub>x</sub> radicals have been proposed, primarily including the formation of HO<sub>2</sub> radicals from the reactions of  $\delta$ -INOO with NO/NO<sub>3</sub>/RO<sub>2</sub>

Received: November 10, 2023 Revised: January 15, 2024 Accepted: January 16, 2024 Published: January 31, 2024





Figure 1. Reaction scheme for the  $HO_x$  radical generation from the  $NO_3$ -initiated oxidation of isoprene. Note that the four INOO radicals could further react with  $NO_3$ , and  $HO_2$  under chamber conditions but only reactions that yield  $HO_x$  radicals are given here.

and the recycling of OH radicals from the  $\beta$ -INOO + HO $_2$  reactions (see pathways highlighted in red in Figure 1). However, the overall production efficiency of HO $_x$  radicals from isoprene nighttime chemistry remains elusive at present. This uncertainty limits our understanding of the overall oxidizing capacity of the nighttime, especially in regions with high vegetation cover densities.

The majority of earlier experimental studies used NO<sub>x</sub> and an excessive amount of  $O_3$  as the  $NO_3$  source, thus resulting in a laboratory environment in the absence of any NO.  $^{17-19,24-29}$ In the actual atmosphere, however, tens to hundreds of pptv levels of NO have been observed over forest sites during nighttime, <sup>13,23,30</sup> and the NO concentrations can be as high as a few ppb in areas impacted by intensive human activities and fire emissions.<sup>13</sup> As NO plays a governing role in converting  $HO_2$  to OH radicals (NO +  $HO_2 \rightarrow OH + NO_2$ ), a chamber environment in the presence of an atmospherically relevant amount of NO is essential in order to reproduce the radical recycling chemistry in an actual nocturnal atmosphere. In this work, we reexamined the nighttime chemistry of isoprene with chamber experiments operated in the continuous-flow steadystate mode. By precisely controlling the inlet reactant concentrations and the ratio of chamber mixing to residence time scales, a chemical regime that features sub-ppbv levels of steady-state NO was created, allowing for an accurate representation of the nighttime oxidation processes in regions with intertwined biogenic and anthropogenic activities. Instead of directly measuring the OH mixing ratios that are often subject to various interferences, we used the measurements of steady-state trace levels of cyclohexane to derive the overall OH production from the NO<sub>3</sub>-initiated oxidation of isoprene. With a simplified mechanism that captures our chamber observations, we predicted that the mixing ratios of OH radicals can exceed  $\sim 10^5$  molecules cm<sup>-3</sup> in the presence of sub-ppb levels of isoprene and NO. Such an efficient production of OH radicals can have an important impact on the oxidizing power of the nocturnal atmosphere disturbed by biomass burning emissions.

# 2. METHODS

**2.1. Chamber Experiments.** Experiments were conducted in a 10 m<sup>3</sup> NCAR Atmospheric Simulation Chamber. <sup>31,32</sup> Prior to each experiment, the chamber was flushed with purified dry

air from an ultrahigh purity zero air generator (Model 737, Aadco Instruments) for >12 h until ozone and NO<sub>x</sub> levels were below 1 ppb. During the operation of the continuous-flow steady-state mode, the chamber was constantly flushed with purified dry air at 50 L min<sup>-1</sup>, which resulted in an average chamber residence time of  $\sim$ 3.3 h. The incoming and outgoing flows were balanced by a feedback control system that maintains a constant internal pressure that is  $1.2-4.9 \times 10^{-4}$ atm above ambient. An airflow with diluted isoprene (12-20 ppb) and cyclohexane (3-5 ppb) was continuously flowing through the chamber for >12 h to establish an initial level of the parent hydrocarbons. To mimic the nighttime chemistry in the continuous flow mode, a steady-state NO<sub>3</sub> mixing ratio was created by constantly flowing diluted O3 and NO air through the chamber (NO + O<sub>3</sub>  $\rightarrow$  NO<sub>2</sub> + O<sub>2</sub>; NO<sub>2</sub>+O<sub>3</sub>  $\rightarrow$  NO<sub>3</sub> + O<sub>2</sub>). O<sub>3</sub> was produced by photolyzing O<sub>2</sub> in air at 185 nm using a mercury "Pen-Ray" lamp (UVP LLC, CA). Ozone concentration in the injection flow can be controlled automatically by adjusting the mercury lamp duty cycle. Constant NO injection flow was achieved by diluting the gas flow from a concentrated NO cylinder (NO = 133.16 ppm, balance  $N_2$ ).  $O_3$  was monitored by absorption spectroscopy (Model 49, Thermo Scientific). NO, was monitored by chemiluminescence (Model CLD 88Y, Eco Physics). In addition, a customized highsensitivity chemiluminescence monitor with a detection limit of ~25 ppt was used to detect NO at sub-ppb levels. Mixing ratios of isoprene and cyclohexane were measured by using a gas chromatograph with a customized cryogenic concentrator and a flame ionization detector (GC-FID, Model G1530A, Agilent).

**2.2. Box Modeling.** Reaction kinetics and mechanisms for the gas-phase chemistry were extracted from the Master Chemical Mechanism (MCMv3.3.1, accessible at <a href="http://mcm.york.ac.uk">http://mcm.york.ac.uk</a>). The inorganic reaction scheme includes 21 species and 48 reactions; the isoprene oxidation system includes 611 species and 1974 reactions; and the cyclohexane oxidation system includes 439 species and 1365 reactions. The isoprene nighttime chemistry was modified based on the Caltech isoprene mechanism (CIM), see the list of reactions in Table S1 in the Supporting Information. The kinetic schemes were implemented in Igor8.0 (Wavemetrics) to simulate the temporal profile of a given species *i* in the chamber operated at the continuous-flow steady-state mode:

$$\frac{\mathrm{d}C_i}{\mathrm{d}t} \cdot \tau = C_{i,0} + P_i - C_i - \sum_i k_i \cdot \tau \cdot C_i \tag{1}$$

where  $C_i$  (molecules cm<sup>-3</sup>) is the gas-phase concentration of species i in the well-mixed core of the chamber;  $C_{i,0}$  (molecules  $cm^{-3}$ ) is the initial gas-phase concentration of species i in the injection flow;  $k_i$  (s<sup>-1</sup>) is the pseudo-first-order rate coefficient of a chemical reaction that consumes species i;  $\tau$  (s) is the chamber mean residence time and can be calculated as the total chamber volume divided by the incoming/outgoing flow rate; and  $P_i$  (molecules cm<sup>-3</sup>) is the increment in the concentration of species i through chemical production during one residence time. Note that two terms are neglected in eq 1, i.e., organic vapor condensation into particles and deposition onto chamber walls. This is a reasonable simplification here owing to the relatively high volatilities and low concentrations of the VOCs studied. Nevertheless, the incorporation of these two terms into eq 1 is feasible given the vapor pressure of species i, suspended particle size distributions, gas-particle and gas-wall partitioning coefficients, accommodation coefficients of species i onto particles and walls, and the effective absorbing organic masses on the walls.<sup>33–37</sup> Model input parameters for all simulations include temperature (295 K), local pressure  $(8.6 \times 10^4 \text{ Pa})$ , relative humidity (8%), chamber mean residence time (3.33 h), and input mixing ratios of NO  $(\sim 30-55 \text{ ppb})$ , O<sub>3</sub>  $(\sim 30-360 \text{ ppb})$ , isoprene  $(\sim 10-22 \text{ ppb})$ , and cyclohexane ( $\sim$ 3–5 ppb). The box model was initialized using measured experimental conditions and propagated independently for a 30 h duration for each experiment.

# 3. RESULTS AND DISCUSSION

3.1. Cyclohexane Degradation as an Indicator of the OH Production from Isoprene Nighttime Chemistry. We performed a series of continuous-flow steady-state experiments using the degradation kinetics of cyclohexane to determine the overall HO<sub>x</sub> production efficiency from the NO<sub>3</sub>-initiated oxidation of isoprene. Figure 2 shows the observed temporal profiles of  $NO_x$ ,  $O_3$ , isoprene  $(C_5H_8)$ , and cyclohexane  $(C_6H_{12})$  in a typical ~30 h duration experiment. The first initial steady state was established by continuously flowing 21.4 ppb of isoprene, 3.6 ppb of cyclohexane, and 34.7 ppb of NO through the chamber for >12 h (time series not given in Figure 2). An outgoing flow at 50 L min<sup>-1</sup> continuously withdrawn air from the chamber to balance the internal pressure close to the ambient. Reactions were initiated when an additional ozone airflow was continuously injected into the chamber, providing a supply of NO<sub>3</sub> radicals through reactions with NO<sub>x</sub>. After a short period of ozone generator equilibration, chamber mixing, and successive NO conversion to NO<sub>3</sub>, the concentration of cyclohexane started to decrease, indicating the generation of HO<sub>r</sub> radicals from the NO<sub>3</sub>-initiated oxidation of isoprene. Isoprene decay is faster than cyclohexane due to oxidation by predominantly NO<sub>3</sub> and OH to a much lesser extent. Upon nearly 9 h of reactions, a final steady state was established as evidenced by the constant levels of both reactants and products observed in the chamber.

When experiments were performed in the continuously mixed flow mode, the concentration of any given species in the well-mixed chamber is governed by their input and output fluxes as well as the chemical production and removal processes. For the hydrocarbon precursor cyclohexane, its mass conservation is given by

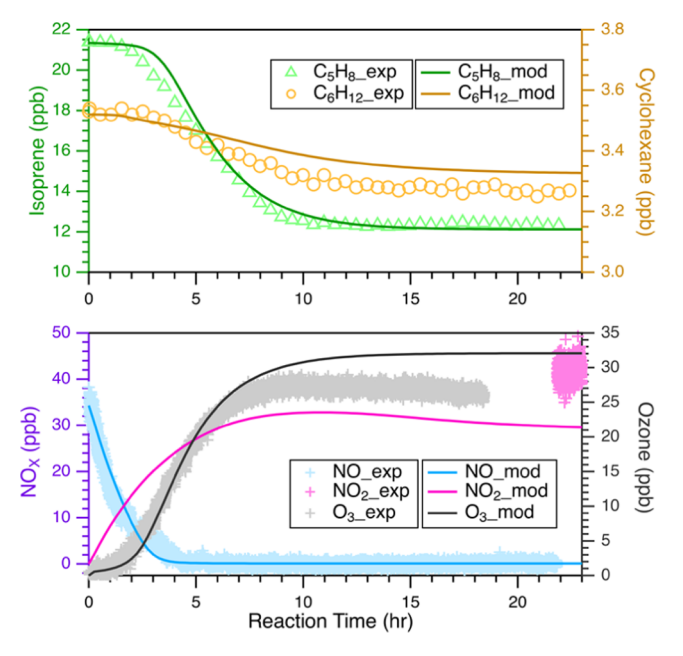


**Figure 2.** Observed and simulated temporal profiles of  $NO_{sv}$   $O_3$ , isoprene, and cyclohexane during a typical 36 h continuous-flow steady-state experiment. The first 10 h for establishing the initial levels of reactants is not shown. Time zero denotes the onset of the reaction initiated by continuously flowing diluted  $O_3$  air through the chamber.

$$\frac{\mathrm{d}[C_6 H_{12}]_{ss}}{\mathrm{d}t} = [C_6 H_{12}]_0 / \tau - [C_6 H_{12}]_{ss} / \tau - k_{C_6 H_{12} + OH}$$

$$\cdot [OH]_{ss} \cdot [C_6 H_{12}]_{ss}$$

$$= 0$$
(2)

where  $[C_6H_{12}]_0$  is the GC-FID measured concentration of cyclohexane at the onset of the experiment,  $[C_6H_{12}]_{ss}$  is the GC-FID measured concentration of cyclohexane upon the establishment of the final steady state, and  $\tau$  is the chamber mean residence time. Note that the NO<sub>3</sub>-initiated oxidation accounts for less than ~1% of the total oxidized mass of cyclohexane at steady state and is neglected here. Rearranging eq 2 yields the steady-state concentration of the OH radicals:

$$[OH]_{ss} = \frac{[C_6 H_{12}]_0 - [C_6 H_{12}]_{ss}}{k_{C_6 H_{12} + OH} \cdot [C_6 H_{12}]_{ss} \cdot \tau}$$
(3)

Uncertainties in the calculated steady-state OH radical concentrations mainly arise from the systematic uncertainties in the GC measurements. These individual uncertainties are further propagated using the variance formula to yield the overall uncertainties in the calculated OH concentrations, as shown in Figure 3. Note that although measurements of cyclohexane can be used to calculate the steady-state OH concentrations, as cyclohexane was exclusively oxidized by OH radicals in the experiments performed, cyclohexane itself is not a governing chemical factor at play in the overall OH radical dynamics, as discussed in Section 3.3.

**3.2.** Model Underestimates the OH Production from NO<sub>3</sub> Oxidation of Isoprene. Figure 3 displays the chamberderived OH mixing ratios given in eq 3 as a function of the NO<sub>3</sub> mixing ratios at steady state, which is approximated as

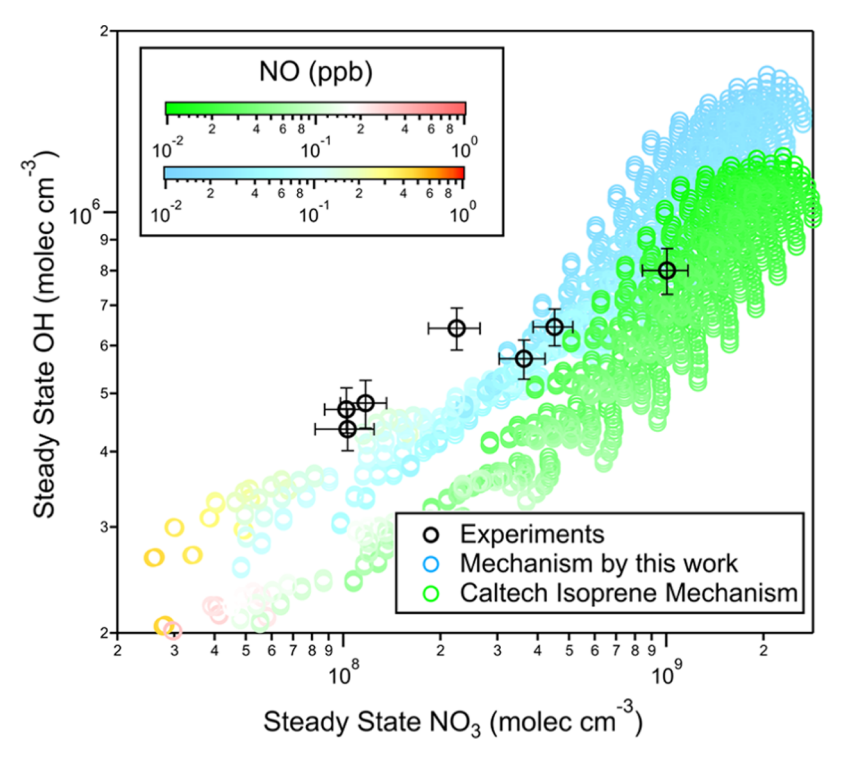


Figure 3. Comparison of chamber-derived steady-state mixing ratios of OH radicals produced from the NO<sub>3</sub>-initiated oxidation of isoprene with corresponding box model simulations.

$$[NO_{3}]_{ss} \approx (k_{O_{3}+NO_{2}} \cdot [O_{3}]_{ss} \cdot [NO_{2}]_{ss})$$

$$/(k_{C_{5}H_{8}+NO_{3}} \cdot [C_{5}H_{8}]_{ss} + k_{NO+NO_{3}} \cdot [NO]_{ss}$$

$$+ k_{N_{2}O_{5}} \cdot K_{NO_{3} \leftrightarrow N_{2}O_{5}} \cdot [NO_{2}]_{ss} + 1/\tau)$$
(4)

where  $k_{O_3+NO_3}$ ,  $k_{NO+NO_3}$ , and  $k_{C_5H_8+NO_3}$  are the rate constants for the O<sub>3</sub>+NO<sub>2</sub>, NO+NO<sub>3</sub>, and C<sub>5</sub>H<sub>8</sub>+NO<sub>3</sub> reactions, respectively,  $K_{N_2O_5\leftrightarrow NO_3}$  is the equilibrium constant for the NO<sub>3</sub> +  $NO_2 + M \leftrightarrow N_2O_5 + M$  reaction, and  $k_{N_2O_5}$  stands for the firstorder removal rate of N2O5 dominated by the outflow dilution and losses to chamber walls. Figure 3 shows the model simulations of steady-state OH vs NO<sub>3</sub> under a broader range of chamber-relevant conditions. Both chamber measurements and model simulations capture the positive correlation between OH and NO<sub>3</sub>, indicating that the isoprene nighttime chemistry is the driving force for HO<sub>x</sub> production and cycling. Chamber measurements, in general, yield higher OH levels by ~14-67% compared with the model simulations under identical conditions. In the Caltech isoprene mechanism, OH radicals are primarily produced through three reaction channels: (1) half of an OH molecule produced per one  $HO_2$  molecule consumed via the reaction with a  $\beta$ -INOO radical, (2) formation of HO<sub>2</sub> radicals with an 80% yield from the  $\delta$ -INOO + NO reaction, and (3) formation of HO<sub>2</sub> radicals at a yield of 100% from the  $\delta$ -INOO + NO<sub>3</sub> reaction, as shown in Figure 1. The HO<sub>2</sub> radicals generated through channels (2) and (3) are readily converted to OH radicals by reacting with NO. In addition to these channels that directly yield HO<sub>x</sub> radicals, formaldehyde generated from the decomposition of  $\beta$ -INO radicals undergoes further reactions with NO<sub>3</sub> producing HO<sub>2</sub> radicals (NO<sub>3</sub> + CH<sub>2</sub>O + O<sub>2</sub>  $\rightarrow$  $HNO_3 + HO_2 + CO$ ). Note that the contribution of INOO + RO<sub>2</sub> reactions to the production of HO<sub>2</sub> radicals is negligible under the conditions investigated here. Our chamber experiments suggest that these channels alone are likely insufficient to sustain the observed OH radical production. Furthermore, the larger model-measurement disagreement under moderate-to-high NO conditions (NO > 0.1 ppb) implies that the current mechanism might underestimate the yield of  $\rm HO_2$  radicals that are available for the  $\rm HO_2$  to OH conversion through reactions with NO.

To match the chamber observations, we revised the mechanism by assuming the INOO + NO reaction leads to HO<sub>2</sub> at a 100% yield and incorporating this reaction pathway into the fate of all four  $\beta/\delta$ -INOO isomers, as shown in Table S2 in the Supporting Information. The updated mechanism not only leads to a closer agreement with the measurements by up to ~29% but also captures the NO dependence of the OH production, as shown in Figure 3. It is important to note that predictions under low NO conditions (NO < 0.1 ppb) are not significantly impacted by the revised mechanism, because the added HO<sub>2</sub> production from INOO + NO is largely offset by the enhanced  $\beta$ -INOO+HO<sub>2</sub> route as an HO<sub>x</sub> sink. Overall, the improved model measurement comparison implies a potential missing scheme for the HO<sub>x</sub> generation, and/or the kinetics of the three existing pathways ( $\beta$ -INOO + HO<sub>2</sub>  $\rightarrow$  0.5· OH,  $\delta$ -INOO + NO  $\rightarrow$  0.8·HO<sub>2</sub>, and  $\delta$ -INOO + NO<sub>3</sub>  $\rightarrow$ HO<sub>2</sub>) needs to be further constrained. A major uncertainty in the current understanding of the isoprene nighttime chemistry is the dynamics of the INOO isomers and their subsequent fates. It is likely that the INOO radicals undergo interconversion through the repetitive addition/removal of O<sub>2</sub> similar to the mechanism discovered in the isoprene photochemistry. 32,38 Such an interconversion, if competing with other bimolecular and unimolecular reactions of INOO radicals, could alter and even control the distribution of INOO isomers and the resulting products. The data set obtained here

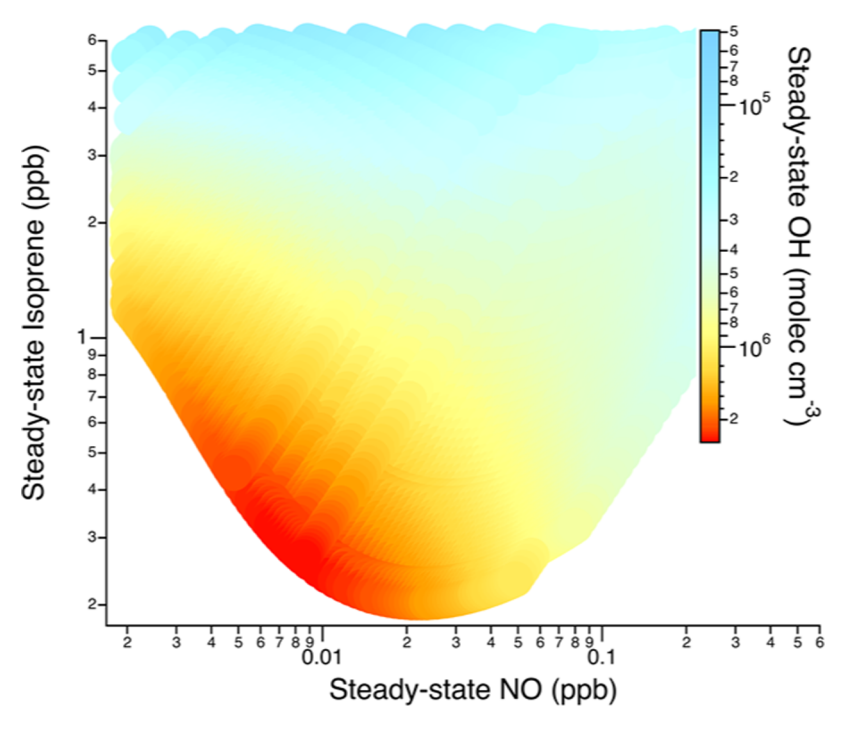


Figure 4. Model simulated steady-state mixing ratios of OH radicals as a function of the steady-state isoprene and NO concentrations under a range of chamber-relevant conditions.

serves to validate reaction pathways that affect the overall  $HO_x$  production efficiency at a range of sub-ppb NO levels.

3.3. Factors Affecting the OH Production Efficacy from Isoprene Nighttime Chemistry in Chamber Experiments. Here, we explore the optimal chamber environment that favors HO<sub>x</sub> production using model simulations with the simplified isoprene mechanism proposed in Section 3.2. Figure 4 displays the OH contour diagram over a range of steady-state levels of isoprene and NO established under simulated chamber conditions. The general trend is evident that a concurrent decrease in both isoprene and NO at steady state leads to a rising level of OH. In other words, increasing the amount of isoprene and NO reacted as a result of the enhanced availability of NO<sub>3</sub> promotes the overall OH production. Given the initial model inputs, i.e., >3 ppb NO and >10 ppb isoprene, the resulting sub-ppb levels of both reactants at steady state signify a strong oxidative environment. At a given NO level, the concentration of O<sub>3</sub> in the incoming flow, which is always in excess, determines the steady-state concentrations of NO<sub>3</sub> and NO<sub>x</sub>. Increasing the inflow O<sub>3</sub> to NO ratio leads to a rising NO<sub>3</sub> but reduced NO and NO<sub>2</sub>. The elevated NO<sub>3</sub> radicals initiate more isoprene oxidation, thereby accumulating more OH radicals. Note that although reactions of ozone with isoprene also yield OH through the vinylhydroperoxide chemistry,<sup>39</sup> the ozonolysis pathway is much less competitive in funneling the isoprene carbon (less than 4.38%) compared with the NO<sub>3</sub> oxidation route under the conditions investigated here.

The total  $HO_x$  level is dynamically balanced by their production from the  $NO_3$  oxidation of isoprene and their removal through reactions with predominantly  $NO_2$ ,  $O_3$ , and isoprene:

$$\begin{split} [\text{OH}]_{\text{ss}} \approx & \\ & \frac{Y_{\text{OH}} \cdot k_{\text{C}_5 \text{H}_8 + \text{NO}_3} \cdot [\text{C}_5 \text{H}_8]_{\text{ss}} \cdot [\text{NO}_3]_{\text{ss}}}{k_{\text{C}_3 \text{H}_8 + \text{OH}} \cdot [\text{C}_5 \text{H}_8]_{\text{ss}} + k_{\text{NO}_2 + \text{OH}} \cdot [\text{NO}_2]_{\text{ss}} + k_{\text{O}_3 + \text{OH}} \cdot [\text{O}_3]_{\text{ss}} + 1/\tau} \end{split} \tag{5}$$

where  $k_{\rm C_3H_8+OH}$ ,  $k_{\rm NO_2+OH}$  and  $k_{\rm O_3+OH}$  are the rate constants for  ${\rm C_5H_8}$  + OH, NO<sub>2</sub> + OH, and O<sub>3</sub> + OH reactions, respectively, and  ${\rm Y}_{\rm OH}$  is the total yield of OH radicals from the cascade of chemistry following the NO<sub>3</sub>-initiated oxidation of isoprene. Cyclohexane accounts for less than 3.7% of the total OH sink and is thereby neglected here. Note that both eqs 3 and 5 express the steady-state OH concentrations, but values of  ${\rm [OH]_{ss}}$  can be only derived from eq 3 since the term  ${\rm Y}_{\rm OH}$  in eq 5 is unknown. It is worth noting that the steady-state OH concentration is no longer sensitive to any NO variation at elevated levels of isoprene ( ${\rm [C_5H_8]_{ss}}$  > 2 ppb). When there is an ample supply of isoprene due to a limited amount of O<sub>3</sub> (and therefore NO<sub>3</sub>) available, the dominant sink of OH radical is to react with isoprene, and thus, eq 5 can be simplified as

$$[OH]_{ss} \approx \frac{Y_{OH} \cdot k_{C_{S}H_{8} + NO_{3}} \cdot [NO_{3}]_{ss}}{k_{C_{S}H_{8} + OH}}$$
(6)

The underlying mechanism is that variations in the steady-state isoprene concentration have an equally important impact on both OH production from the  $NO_3$  oxidation of isoprene and OH removal via reactions with isoprene. As shown in eq 6,  $[OH]_{ss}$  is approximated as an exclusive function of  $[NO_3]_{ss}$ . Any increase in the steady-state  $NO_3$  level is always accompanied by a decrease in the steady-state NO as more NO is consumed by  $O_3$  and  $NO_3$ . While decreasing NO limits the carbon flow going through the  $RO_2$  + NO channel and hinders the conversion of  $HO_2$  to OH through  $HO_2$  + NO reactions, the simultaneous increase in  $NO_3$ , on the other hand, enhances the formation of OH radicals by oxidizing

more isoprene. As a result, variations in NO have a minimal influence on the steady-state OH level in this region, unless accompanied by a concurrent change in the steady-state isoprene.

#### 4. ATMOSPHERIC SIGNIFICANCE

With the updated mechanism that adequately captures our chamber measurements, we predicted the nocturnal mixing ratios of OH radicals at isoprene and  $NO_x$  levels typical of the ambient air impacted by fire plumes  $(0.01-1.0 \text{ ppb} \text{ of isoprene}, 0.01-1.0 \text{ ppb of NO}, \text{ and 10 ppb of O}_3)$ , as shown in Figure 5. It is important to note that the model

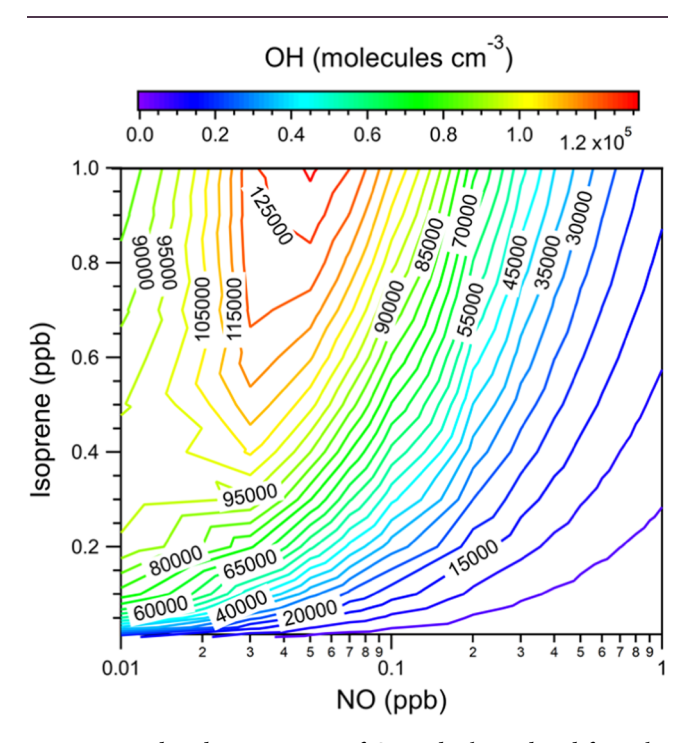


**Figure 5.** Predicted mixing ratios of OH radicals produced from the isoprene nighttime chemistry under a range of NO and isoprene levels typical of air masses under strong biomass burning influences.

configurations for the ambient predictions are intrinsically different from those used for simulating chamber experiments. In particular, cyclohexane was a model input only for simulating chamber experiments, as this compound serves as a tracer to derive the total OH amount produced from the NO<sub>3</sub> oxidation of isoprene. Furthermore, for the ambient predictions, concentrations of all reactants (e.g., isoprene, NO, and O<sub>3</sub>) were held constant throughout the course of individual model runs, whereas for chamber simulations, only inflow concentrations of reactants (including O3, NO, isoprene, and cyclohexane) were held constant, and these reactants, upon mixing in the chamber, were consumed within hours to establish a final steady-state level. This is why the final steady-state mixing ratios of OH radicals in the chamber depend on the amount of isoprene reacted, that is, OH mixing ratios increase with reduced steady-state isoprene levels; see the scatter plot given in Figure 3. In the actual atmosphere, on the other hand, rising isoprene concentrations, in fact, promote the production of OH radicals, as shown in Figure 5.

Simulated OH mixing ratios can reach up to  $1.3 \times 10^5$  molecules cm<sup>-3</sup> in the presence of hundreds of parts per trillion levels of NO and isoprene, with an estimated lifetime of

less than a second. This regime also maximizes the production of NO<sub>3</sub> radicals (>10<sup>8</sup> molecules cm<sup>-3</sup>). It is evident that enhanced emissions of NO and isoprene, together with the presence of elevated ozone, are essential prerequisites for the efficient production of OH radicals at nighttime. Biomass burning, either prescribed or wildfires, is likely the dominant contributor to the rapid accumulation of both isoprene and NO<sub>x</sub> in the nocturnal atmosphere. Our recent study has found that open-land burning of crop residues often produces ppb levels of isoprene and NO<sub>x</sub> at night during the harvest season in rural China. Such a holistic emission that synchronously releases both biogenic hydrocarbons and anthropogenic pollutants and the impact of ensuing chemistry on the composition of the nighttime atmosphere have not yet been thoroughly understood. Results from this study provide insights into the radical cycling and oxidizing power of the atmosphere at night under heavy influences from biomass burning emissions.

#### ASSOCIATED CONTENT

# Supporting Information

The Supporting Information is available free of charge at https://pubs.acs.org/doi/10.1021/acsearthspace-chem.3c00323.

Isoprene reactions in MCM based on the Caltech isoprene mechanism (PDF)

#### AUTHOR INFORMATION

#### **Corresponding Author**

Xuan Zhang — Department of Life and Environmental Sciences, University of California, Merced, California 95343, United States; orcid.org/0000-0003-1548-8021; Email: xzhang87@ucmerced.edu

#### **Authors**

Zeyi Moo – Department of Life and Environmental Sciences, University of California, Merced, California 95343, United States; orcid.org/0009-0004-6621-5220

Peizhi Hao – Department of Life and Environmental Sciences, University of California, Merced, California 95343, United States

Kate E. DeMarsh – Department of Life and Environmental Sciences, University of California, Merced, California 95343, United States

Complete contact information is available at: https://pubs.acs.org/10.1021/acsearthspacechem.3c00323

# Notes

The authors declare no competing financial interest.

# ACKNOWLEDGMENTS

The work was supported by the U.S. National Science Foundation Grant AGS-2131199. Helpful discussions with Dr. John Orlando and Dr. Geoff Tyndall are appreciated.

### REFERENCES

- (1) Ng, N. L.; Brown, S. S.; Archibald, A. T.; Atlas, E.; Cohen, R. C.; Crowley, J. N.; Day, D. A.; Donahue, N. M.; Fry, J. L.; Fuchs, H.; et al. Nitrate radicals and biogenic volatile organic compounds: oxidation, mechanisms, and organic aerosol. *Atmos. Chem. Phys.* **2017**, *17* (3), 2103–2162.
- (2) Penkett, S. A.; Blake, N. J.; Lightman, P.; Marsh, A. R. W.; Anwyl, P.; Butcher, G. The seasonal variation of nonmethane

- hydrocarbons in the free troposphere over the North Atlantic Ocean: Possible evidence for extensive reaction of hydrocarbons with the nitrate radical. *J. Geophys. Res.: Atmos.* **1993**, 98 (D2), 2865–2885.
- (3) Penkett, S. A.; Burgess, R. A.; Coe, H.; Coll, I.; Hov, Ø.; Lindskog, A.; Schmidbauer, N.; Solberg, S.; Roemer, M.; Thijsse, T.; et al. Evidence for large average concentrations of the nitrate radical (NO3) in Western Europe from the HANSA hydrocarbon database. *Atmos. Environ.* **2007**, *41* (16), 3465–3478.
- (4) Guenther, A.; Karl, T.; Harley, P.; Wiedinmyer, C.; Palmer, P. I.; Geron, C. Estimates of global terrestrial isoprene emissions using MEGAN (Model of Emissions of Gases and Aerosols from Nature). *Atmos. Chem. Phys.* **2006**, *6* (11), 3181–3210.
- (5) Brown, S. S.; Stutz, J. Nighttime radical observations and chemistry. Chem. Soc. Rev. 2012, 41 (19), 6405–6447.
- (6) Harley, P.; Vasconcellos, P.; Vierling, L.; Pinheiro, C. C. d. S.; Greenberg, J.; Guenther, A.; Klinger, L.; Almeida, S. S. d.; Neill, D.; Baker, T.; et al. Variation in potential for isoprene emissions among Neotropical forest sites. *Global Change Biol.* **2004**, *10* (5), 630–650.
- (7) Sharkey, T. D.; Singsaas, E. L.; Vanderveer, P. J.; Geron, C. Field measurements of isoprene emission from trees in response to temperature and light. *Tree Physiol.* **1996**, *16* (7), 649–654.
- (8) Gao, Y.; Wang, H.; Liu, Y.; Zhang, X.; Jing, S.; Peng, Y.; Huang, D.; Li, X.; Chen, S.; Lou, S.; et al. Unexpected High Contribution of Residential Biomass Burning to Non-Methane Organic Gases (NMOGs) in the Yangtze River Delta Region of China. *J. Geophys. Res.: Atmos.* 2022, 127 (4), No. e2021JD035050.
- (9) Decker, Z. C. J.; Zarzana, K. J.; Coggon, M.; Min, K.-E.; Pollack, I.; Ryerson, T. B.; Peischl, J.; Edwards, P.; Dubé, W. P.; Markovic, M. Z.; et al. Nighttime chemical transformation in biomass burning plumes: a box model analysis initialized with aircraft observations. *Environ. Sci. Technol.* **2019**, *53* (5), 2529–2538.
- (10) Brilli, F.; Gioli, B.; Ciccioli, P.; Zona, D.; Loreto, F.; Janssens, I. A.; Ceulemans, R. Proton Transfer Reaction Time-of-Flight Mass Spectrometric (PTR-TOF-MS) determination of volatile organic compounds (VOCs) emitted from a biomass fire developed under stable nocturnal conditions. *Atmos. Environ.* **2014**, 97, 54–67.
- (11) Wang, H.; Gao, Y.; Wang, S.; Wu, X.; Liu, Y.; Li, X.; Huang, D.; Lou, S.; Wu, Z.; Guo, S.; et al. Atmospheric processing of nitrophenols and nitrocresols from biomass burning emissions. *J. Geophys. Res.: Atmos.* **2020**, 125 (22), No. e2020JD033401.
- (12) Brown, S. S.; Degouw, J. A.; Warneke, C.; Ryerson, T. B.; Dubé, W. P.; Atlas, E.; Weber, R. J.; Peltier, R. E.; Neuman, J. A.; Roberts, J. M.; et al. Nocturnal isoprene oxidation over the Northeast United States in summer and its impact on reactive nitrogen partitioning and secondary organic aerosol. *Atmos. Chem. Phys.* **2009**, *9* (9), 3027–3042.
- (13) Stroud, C. A.; Roberts, J. M.; Williams, E. J.; Hereid, D.; Angevine, W. M.; Fehsenfeld, F. C.; Wisthaler, A.; Hansel, A.; Martinez-Harder, M.; Harder, H.; et al. Nighttime isoprene trends at an urban forested site during the 1999 Southern Oxidant Study. *J. Geophys. Res.: Atmos.* 2002, 107 (D16), No. D000959, DOI: 10.1029/2001JD000959.
- (14) Brown, S. S.; Dubé, W. P.; Peischl, J.; Ryerson, T. B.; Atlas, E.; Warneke, C.; De Gouw, J. A.; te Lintel Hekkert, S.; Brock, C. A.; Flocke, F.; et al. Budgets for nocturnal VOC oxidation by nitrate radicals aloft during the 2006 Texas Air Quality Study. *J. Geophys. Res.: Atmos.* 2011, 116 (D24), No. JD016544, DOI: 10.1029/2011JD016544.
- (15) Pye, H. O. T.; Chan, A. W. H.; Barkley, M. P.; Seinfeld, J. H. Global modeling of organic aerosol: The importance of reactive nitrogen (NOx and NO3). *Atmos. Chem. Phys.* **2010**, *10* (22), 11261–11276.
- (16) Skov, H.; Hjorth, J.; Lohse, C.; Jensen, N. R.; Restelli, G. Products and mechanisms of the reactions of the nitrate radical (NO3) with isoprene, 1, 3-butadiene and 2, 3-dimethyl-1, 3-butadiene in air. *Atmos. Environ.*, *Part A* **1992**, *26* (15), 2771–2783.
- (17) Berndt, T.; Böge, O. Gas-phase reaction of NO3 radicals with isoprene: a kinetic and mechanistic study. *Int. J. Chem. Kinet.* **1997**, 29 (10), 755–765.

- (18) Perring, A.; Wisthaler, A.; Graus, M.; Wooldridge, P.; Lockwood, A.; Mielke, L.; Shepson, P.; Hansel, A.; Cohen, R. A product study of the isoprene+ NO 3 reaction. *Atmos. Chem. Phys.* **2009**, 9 (14), 4945–4956.
- (19) Rollins, A. W.; Kiendler-Scharr, A.; Fry, J.; Brauers, T.; Brown, S. S.; Dorn, H.-P.; Dube, W. P.; Fuchs, H.; Mensah, A.; Mentel, T.; et al. Isoprene oxidation by nitrate radical: alkyl nitrate and secondary organic aerosol yields. *Atmos. Chem. Phys.* **2009**, *9* (18), 6685–6703.
- (20) Schwantes, R. H.; Teng, A. P.; Nguyen, T. B.; Coggon, M. M.; Crounse, J. D.; St Clair, J. M.; Zhang, X.; Schilling, K. A.; Seinfeld, J. H.; Wennberg, P. O. Isoprene NO3 oxidation products from the RO2+ HO2 pathway. *J. Phys. Chem. A* **2015**, *119* (40), 10158–10171.
- (21) Platt, U.; LeBras, G.; Poulet, G.; Burrows, J. P.; Moortgat, G. Peroxy radicals from night-time reaction of N03 with organic compounds. *Nature* **1990**, 348, 147–149.
- (22) Geyer, A.; Bächmann, K.; Hofzumahaus, A.; Holland, F.; Konrad, S.; Klüpfel, T.; Pätz, H. W.; Perner, D.; Mihelcic, D.; Schäfer, H. J.; et al. Nighttime formation of peroxy and hydroxyl radicals during the BERLIOZ campaign: Observations and modeling studies. *J. Geophys. Res.: Atmos.* **2003**, *108* (D4), No. D000656, DOI: 10.1029/2001JD000656.
- (23) Ambrose, J. L.; Mao, H.; Mayne, H. R.; Stutz, J.; Talbot, R.; Sive, B. C. Nighttime nitrate radical chemistry at Appledore island, Maine during the 2004 international consortium for atmospheric research on transport and transformation. *J. Geophys. Res.: Atmos.* 2007, 112 (D21), No. D008756, DOI: 10.1029/2007|D008756.
- (24) Kwan, A.; Chan, A.; Ng, N.; Kjaergaard, H.; Seinfeld, J.; Wennberg, P. Peroxy radical chemistry and OH radical production during the NO 3-initiated oxidation of isoprene. *Atmos. Chem. Phys.* **2012**, *12* (16), 7499–7515.
- (25) Wille, U.; Becker, E.; Schindler, R.; Lancar, I.; Poulet, G.; Le Bras, G. A discharge flow mass-spectrometric study of the reaction between the NO3 radical and isoprene. *J. Atmos. Chem.* **1991**, *13*, 183–193.
- (26) Skov, H.; Hjorth, J.; Lohse, C.; Jensen, N.; Restelli, G. Products and mechanisms of the reactions of the nitrate radical (NO3) with isoprene, 1, 3-butadiene and 2, 3-dimethyl-1, 3-butadiene in air. *Atmos. Environ., Part A* **1992**, *26* (15), 2771–2783.
- (27) Kwok, E. S. C.; Aschmann, S. M.; Arey, J.; Atkinson, R. Product formation from the reaction of the NO3 radical with isoprene and rate constants for the reactions of methacrolein and methyl vinyl ketone with the NO3 radical. *Int. J. Chem. Kinet.* **1996**, 28 (12), 925–934.
- (28) Suh, I.; Lei, W.; Zhang, R. Experimental and theoretical studies of isoprene reaction with NO3. *J. Phys. Chem. A* **2001**, *105* (26), 6471–6478.
- (29) Ng, N.; Kwan, A.; Surratt, J.; Chan, A.; Chhabra, P.; Sorooshian, A.; Pye, H. O.; Crounse, J.; Wennberg, P.; Flagan, R. Secondary organic aerosol (SOA) formation from reaction of isoprene with nitrate radicals (NO 3). *Atmos. Chem. Phys.* **2008**, 8 (14), 4117–4140.
- (30) McFarland, M.; Kley, D.; Drummond, J. W.; Schmeltekopf, A. L.; Winkler, R. H. Nitric oxide measurements in the equatorial Pacific region. *Geophys. Res. Lett.* **1979**, *6* (7), 605–608.
- (31) Zhang, X.; Ortega, J.; Huang, Y.; Shertz, S.; Tyndall, G. S.; Orlando, J. J. A steady-state continuous flow chamber for the study of daytime and nighttime chemistry under atmospherically relevant NO levels. *Atmos. Meas. Tech.* **2018**, *11* (5), 2537–2551.
- (32) Zhang, X.; Wang, S.; Apel, E. C.; Schwantes, R. H.; Hornbrook, R. S.; Hills, A. J.; DeMarsh, K. E.; Moo, Z.; Ortega, J.; Brune, W. H.; et al. Probing isoprene photochemistry at atmospherically relevant nitric oxide levels. *Chem* **2022**, *8* (12), 3225–3240.
- (33) Zhang, X.; Cappa, C. D.; Jathar, S. H.; McVay, R. C.; Ensberg, J. J.; Kleeman, M. J.; Seinfeld, J. H. Influence of vapor wall loss in laboratory chambers on yields of secondary organic aerosol. *Proc. Natl. Acad. Sci. U.S.A.* **2014**, *111* (16), 5802–5807.
- (34) Zhang, X.; Schwantes, R. H.; McVay, R. C.; Lignell, H.; Coggon, M. M.; Flagan, R. C.; Seinfeld, J. H. Vapor wall deposition in Teflon chambers. *Atmos. Chem. Phys.* **2015**, *15* (8), 4197–4214.

- (35) Huang, D. D.; Zhang, X.; Dalleska, N. F.; Lignell, H.; Coggon, M. M.; Chan, C. M.; Flagan, R. C.; Seinfeld, J. H.; Chan, C. K. A note on the effects of inorganic seed aerosol on the oxidation state of secondary organic aerosol— $\alpha$ -pinene ozonolysis. *J. Geophys. Res.:* Atmos. **2016**, 121, 12–476, DOI: 10.1002/2016JD025999.
- (36) McVay, R. C.; Zhang, X.; Aumont, B.; Valorso, R.; Camredon, M.; La, Y. S.; Wennberg, P. O.; Seinfeld, J. H. SOA formation from the photooxidation of  $\alpha$ -pinene: systematic exploration of the simulation of chamber data. *Atmos. Chem. Phys.* **2016**, *16* (5), 2785–2802.
- (37) Nah, T.; McVay, R. C.; Zhang, X.; Boyd, C. M.; Seinfeld, J. H.; Ng, N. L. Influence of seed aerosol surface area and oxidation rate on vapor wall deposition and SOA mass yields: a case study with  $\alpha$ -pinene ozonolysis. *Atmos. Chem. Phys.* **2016**, *16* (14), 9361–9379.
- (38) Wennberg, P. O.; Bates, K. H.; Crounse, J. D.; Dodson, L. G.; McVay, R. C.; Mertens, L. A.; Nguyen, T. B.; Praske, E.; Schwantes, R. H.; Smarte, M. D.; et al. Gas-phase reactions of isoprene and its major oxidation products. *Chem. Rev.* **2018**, *118* (7), 3337–3390.
- (39) Nguyen, T. B.; Tyndall, G. S.; Crounse, J. D.; Teng, A. P.; Bates, K. H.; Schwantes, R. H.; Coggon, M. M.; Zhang, L.; Feiner, P.; Milller, D. O.; et al. Atmospheric fates of Criegee intermediates in the ozonolysis of isoprene. *Phys. Chem. Chem. Phys.* **2016**, *18* (15), 10241–10254.